Supplementary Information

Experimental Absence of the Non-Perovskite Ground State Phases of $MaPbI_3$ Explained by a Funnel Hopping Monte Carlo Study Based on a Neural Network Potential

Jonas A. Finkler, Stefan Goedecker

November 8, 2022

Contents

Supercells **2**

Neural Network Potential **7**
Correlation Plots . . . 7
Symmetry Functions . . . 8

DFT Settings **14**

Order Parameter **15**

Funnel Hopping Monte Carlo **15**
Acceptance Rates of MC Moves . . . 15
FHMC Simulation With a Different Lattice Parameters of the Tetragonal Phase . . . 16

Harmonic and Quasi Harmonic Approximation **18**

1 Supercells

We used the same supercells for all FHMC, MD and phonon calculations. Pictures of the supercells for each phase are shown in the figures below.

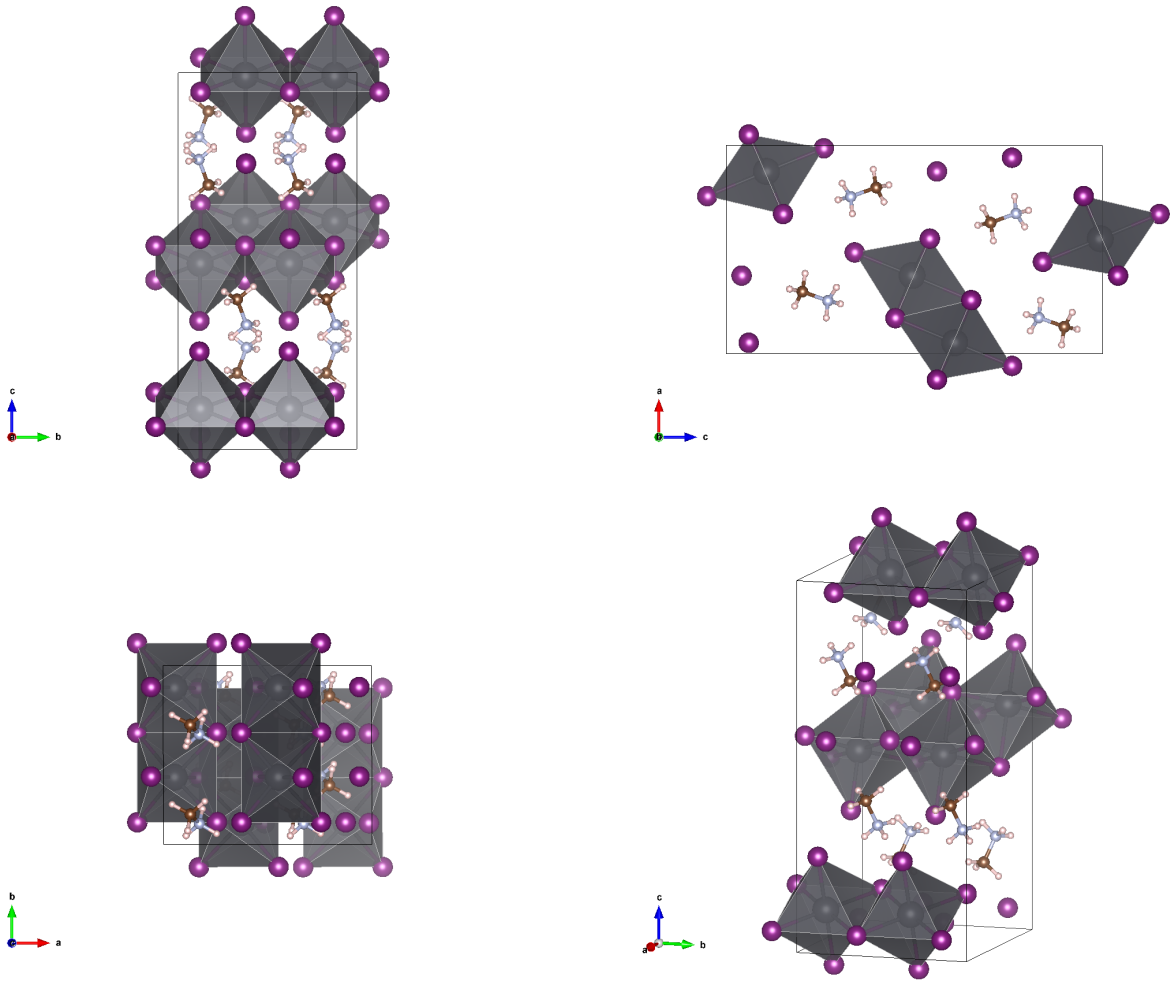

Supplemental Figure 1: Geometry of the supercell used for the double delta phase.

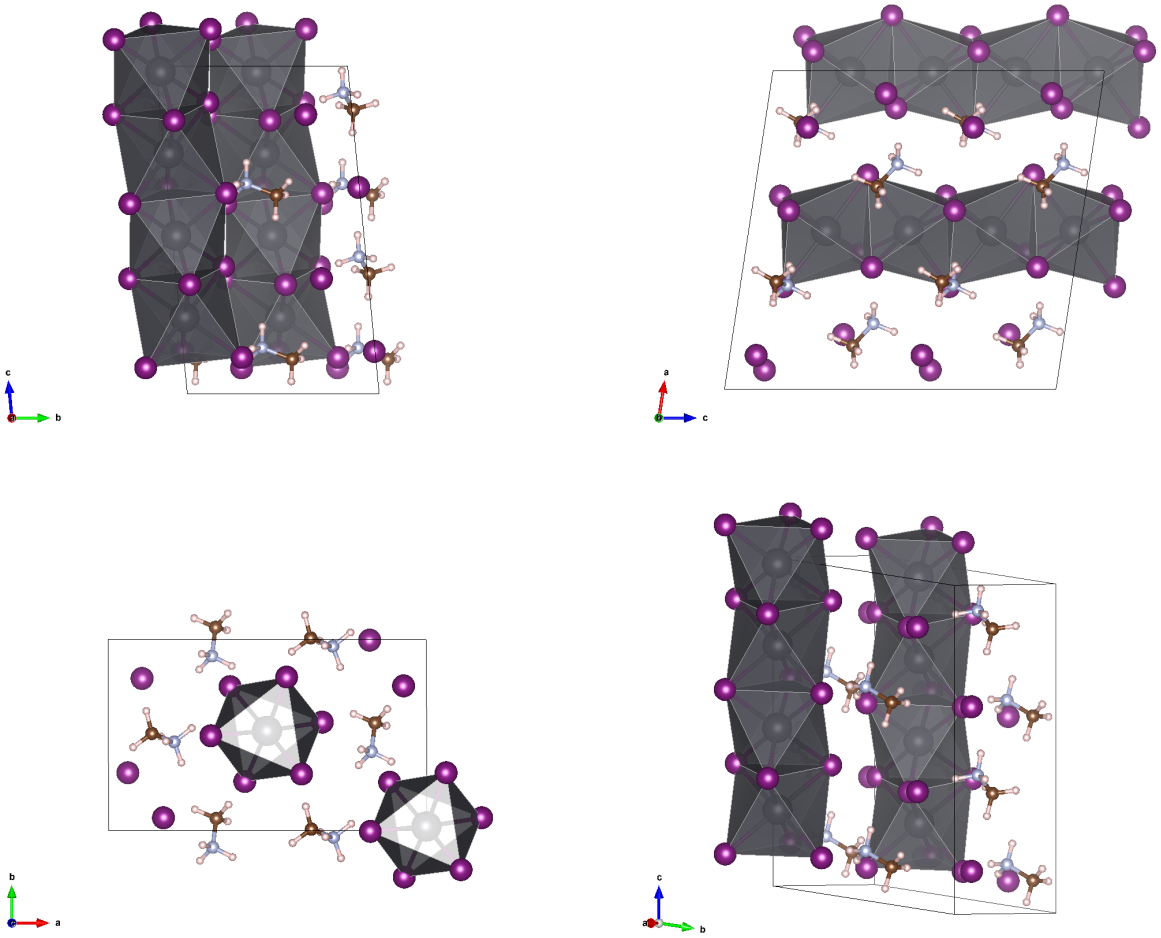

Supplemental Figure 2: Geometry of the supercell used for the delta phase.

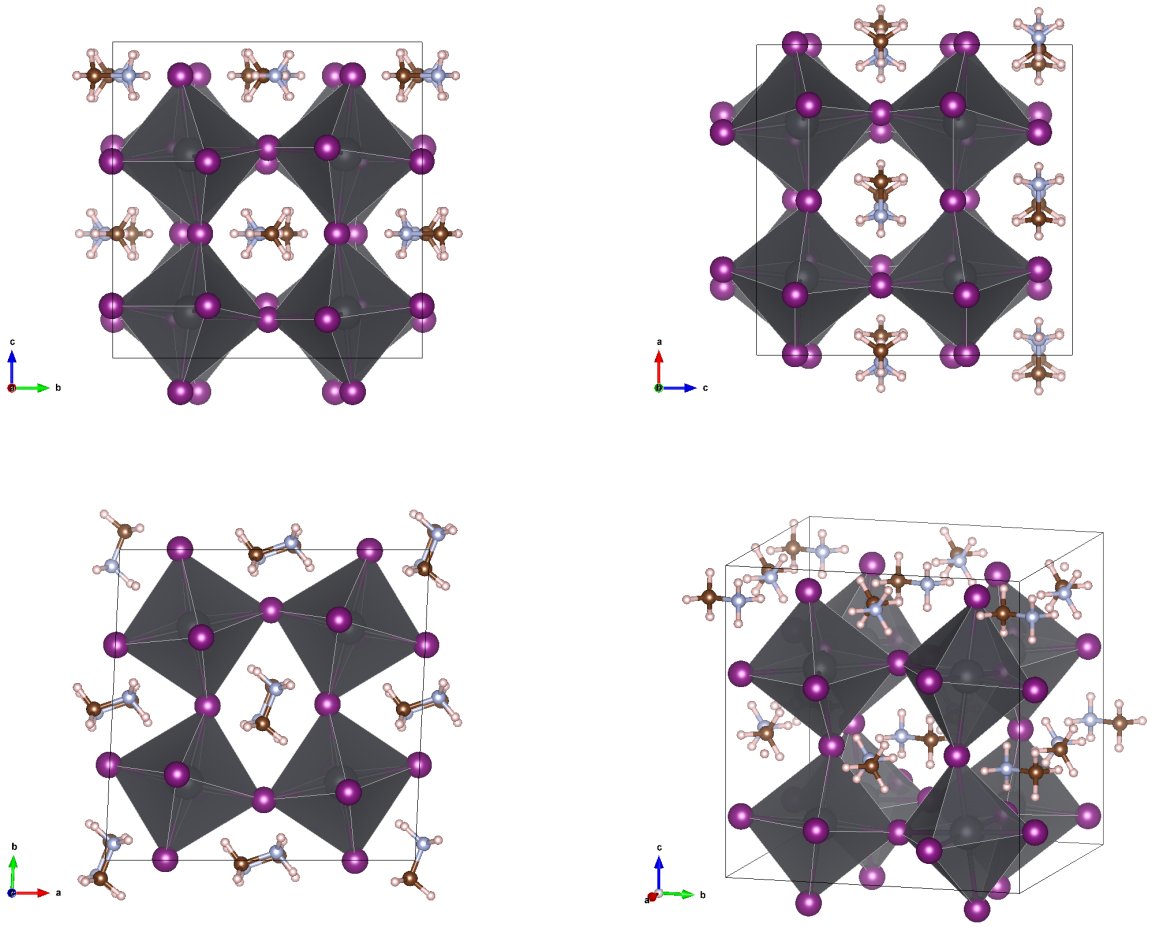

Supplemental Figure 3: Geometry of the supercell used for the orthorhombic phase.

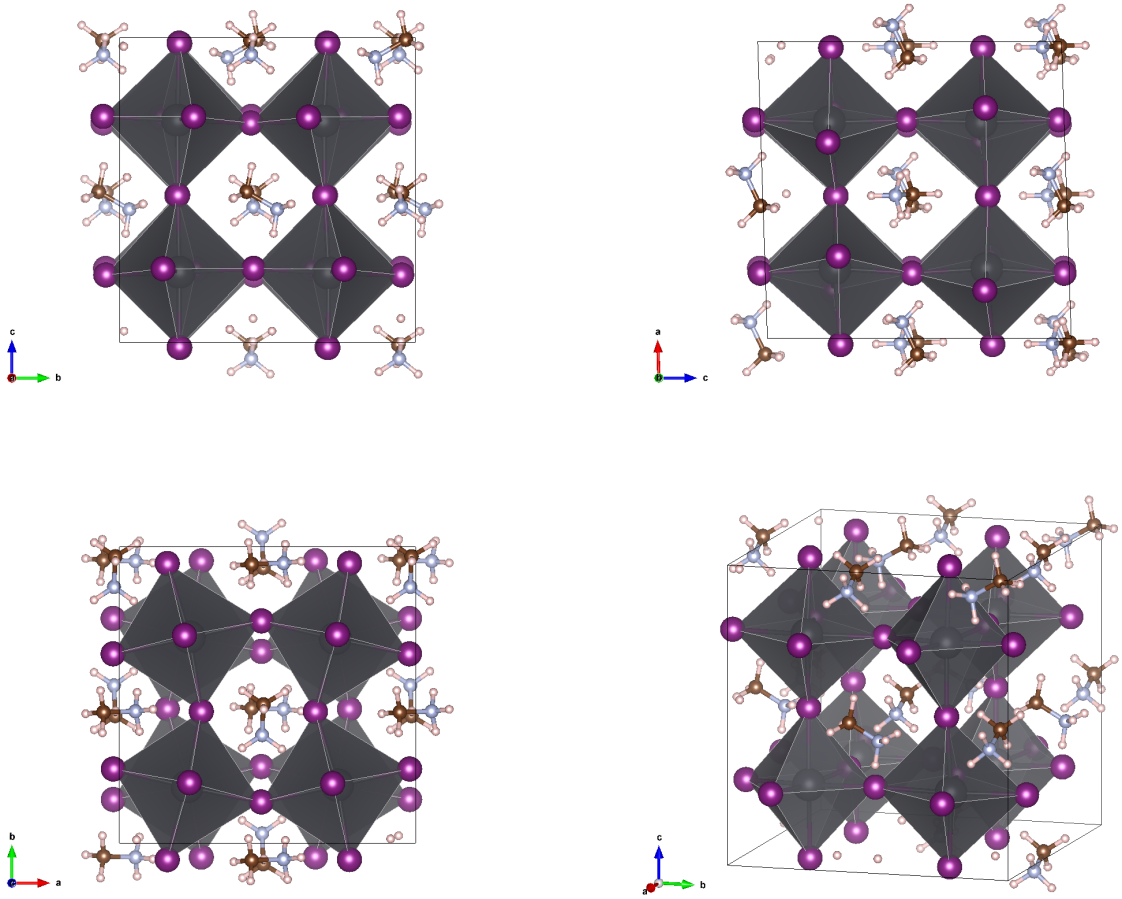

Supplemental Figure 4: Geometry of the supercell used for the tetragonal phase.

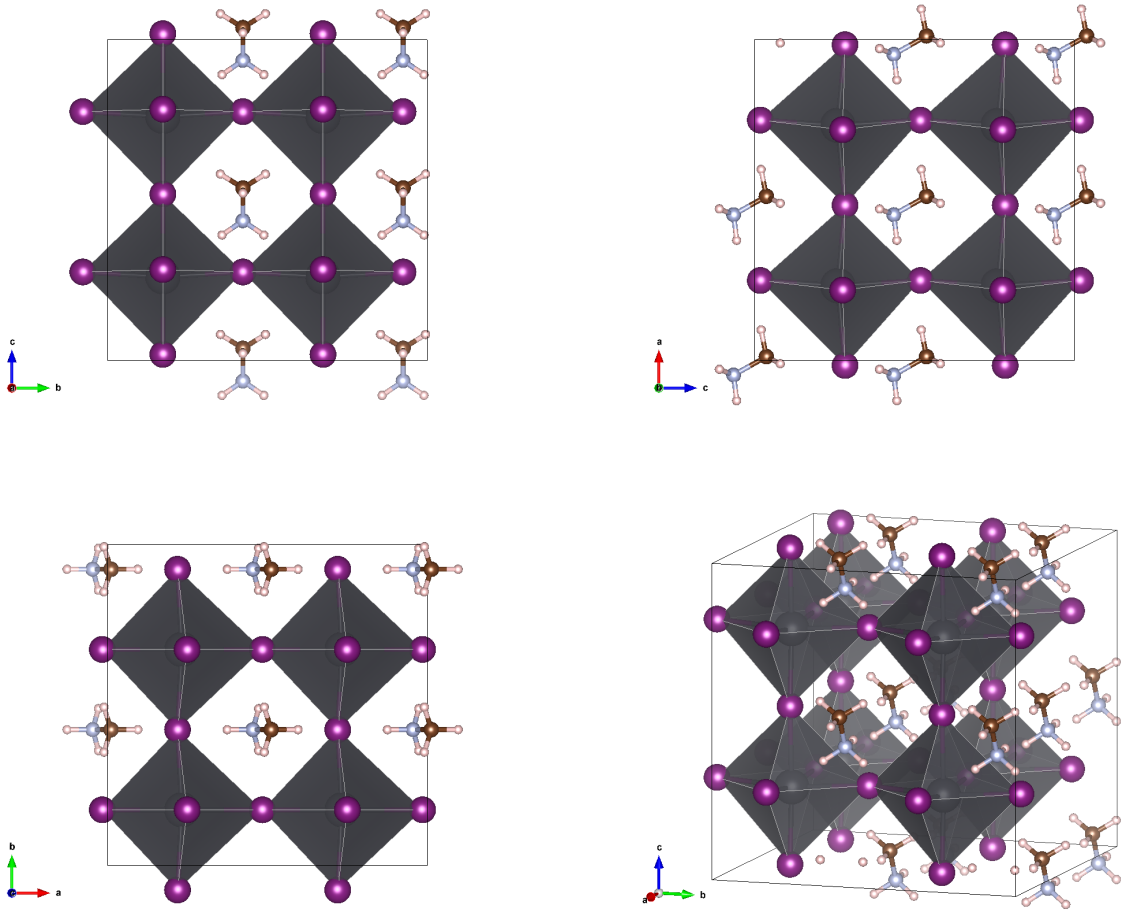

Supplemental Figure 5: Geometry of the supercell used for the cubic phase.

2 Neural Network Potential

2.1 Correlation Plots

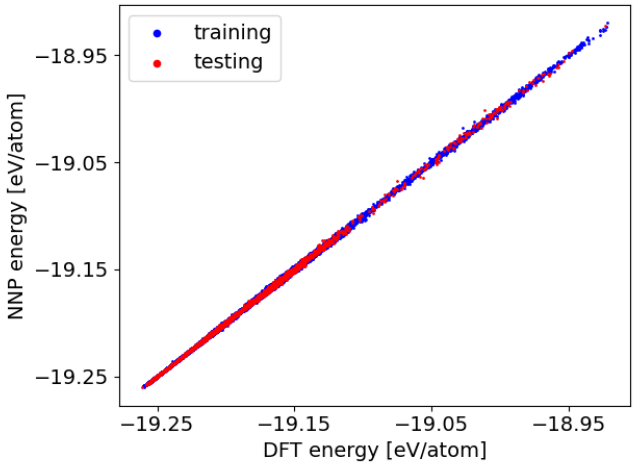

Supplemental Figure 6: Correlation plot of the energy per atom predicted by the NNP versus the reference energies for the training and test data sets.

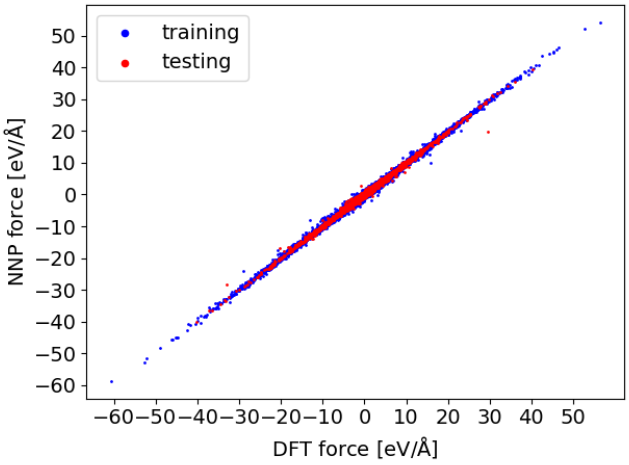

Supplemental Figure 7: Correlation plot of the force components predicted by the NNP versus the reference forces for the training and test data sets.

2.2 Symmetry Functions

We used 2- (G^2) and 3-body (G^4) atom centered symmetry functions [1] as atomic environment descriptors for out neural network potential.

$$G_i^2 = \sum_j e^{-\eta(R_{ij}-R_\mathrm{s})^3} \cdot f_\mathrm{c}(R_{ij}) \tag{1}$$

$$G_i^4 = 2^{1-\zeta} \sum_{j,k\neq i} (1+\lambda\cos(\theta_{ijk}))^\zeta \cdot e^{-\eta(R_{ij}^2+R_{ik}^2+R_{jk}^2)} \cdot f_\mathrm{c}(R_{ij}) \cdot f_\mathrm{c}(R_{ik}) \cdot f_\mathrm{c}(R_{jk}) \tag{2}$$

$$f_\mathrm{c}(R) = \tanh(1-R/R_\mathrm{c})^3 \tag{3}$$

Supplemental Table 1: Symmetry functions used for the neural network potential

no.	type	atom i	atom j	atom k	η(1/Bohr^2)	λ	ζ	R_c(Bohr)	R_s(Bohr)
1	G^2	H	H		0.004			12.0	0.0
2	G^2	H	H		0.028			12.0	0.0
3	G^2	H	H		0.139			12.0	0.0
4	G^2	H	H		0.556			12.0	0.0
5	G^2	H	H		1.000			12.0	0.0
6	G^2	H	C		0.004			12.0	0.0
7	G^2	H	C		0.028			12.0	0.0
8	G^2	H	C		0.139			12.0	0.0
9	G^2	H	C		0.556			12.0	0.0
10	G^2	H	C		1.000			12.0	0.0
11	G^2	H	N		0.004			12.0	0.0
12	G^2	H	N		0.028			12.0	0.0
13	G^2	H	N		0.139			12.0	0.0
14	G^2	H	N		0.556			12.0	0.0
15	G^2	H	N		1.000			12.0	0.0
16	G^2	H	I		0.004			12.0	0.0
17	G^2	H	I		0.028			12.0	0.0
18	G^2	H	I		0.139			12.0	0.0
19	G^2	H	Pb		0.004			12.0	0.0
20	G^2	H	Pb		0.028			12.0	0.0
21	G^2	H	Pb		0.139			12.0	0.0
22	G^4	H	H	H	0.005	−1.0	1.0	12.0	
23	G^4	H	H	H	0.005	−1.0	4.0	12.0	
24	G^4	H	H	H	0.005	1.0	1.0	12.0	
25	G^4	H	H	H	0.005	1.0	4.0	12.0	
26	G^4	H	H	C	0.005	−1.0	1.0	12.0	
27	G^4	H	H	C	0.005	−1.0	4.0	12.0	
28	G^4	H	H	C	0.005	1.0	1.0	12.0	
29	G^4	H	H	C	0.005	1.0	4.0	12.0	
30	G^4	H	H	N	0.005	−1.0	1.0	12.0	
31	G^4	H	H	N	0.005	−1.0	4.0	12.0	
32	G^4	H	H	N	0.005	1.0	1.0	12.0	

no.	type	atom i	atom j	atom k	$\eta(1/\mathrm{Bohr}^2)$	λ	ζ	R_c(Bohr)	R_s(Bohr)
33	G^4	H	H	N	0.005	1.0	4.0	12.0	
34	G^4	H	H	I	0.005	−1.0	1.0	12.0	
35	G^4	H	H	I	0.005	−1.0	4.0	12.0	
36	G^4	H	H	I	0.005	1.0	1.0	12.0	
37	G^4	H	H	I	0.005	1.0	4.0	12.0	
38	G^4	H	H	Pb	0.005	−1.0	1.0	12.0	
39	G^4	H	H	Pb	0.005	−1.0	4.0	12.0	
40	G^4	H	H	Pb	0.005	1.0	1.0	12.0	
41	G^4	H	H	Pb	0.005	1.0	4.0	12.0	
42	G^4	H	C	C	0.005	−1.0	1.0	12.0	
43	G^4	H	C	C	0.005	−1.0	4.0	12.0	
44	G^4	H	C	C	0.005	1.0	1.0	12.0	
45	G^4	H	C	C	0.005	1.0	4.0	12.0	
46	G^4	H	C	N	0.005	−1.0	1.0	12.0	
47	G^4	H	C	N	0.005	−1.0	4.0	12.0	
48	G^4	H	C	N	0.005	1.0	1.0	12.0	
49	G^4	H	C	N	0.005	1.0	4.0	12.0	
50	G^4	H	C	I	0.005	−1.0	1.0	12.0	
51	G^4	H	C	I	0.005	−1.0	4.0	12.0	
52	G^4	H	C	I	0.005	1.0	1.0	12.0	
53	G^4	H	C	I	0.005	1.0	4.0	12.0	
54	G^4	H	C	Pb	0.005	−1.0	1.0	12.0	
55	G^4	H	C	Pb	0.005	−1.0	4.0	12.0	
56	G^4	H	C	Pb	0.005	1.0	1.0	12.0	
57	G^4	H	C	Pb	0.005	1.0	4.0	12.0	
58	G^4	H	N	N	0.005	−1.0	1.0	12.0	
59	G^4	H	N	N	0.005	−1.0	4.0	12.0	
60	G^4	H	N	N	0.005	1.0	1.0	12.0	
61	G^4	H	N	I	0.005	−1.0	1.0	12.0	
62	G^4	H	N	I	0.005	−1.0	4.0	12.0	
63	G^4	H	N	I	0.005	1.0	1.0	12.0	
64	G^4	H	N	I	0.005	1.0	4.0	12.0	
65	G^4	H	N	Pb	0.005	−1.0	1.0	12.0	
66	G^4	H	N	Pb	0.005	−1.0	4.0	12.0	
67	G^4	H	N	Pb	0.005	1.0	1.0	12.0	
68	G^4	H	I	I	0.005	−1.0	1.0	12.0	
69	G^4	H	I	I	0.005	−1.0	4.0	12.0	
70	G^4	H	I	I	0.005	1.0	1.0	12.0	
71	G^4	H	I	I	0.005	1.0	4.0	12.0	
72	G^4	H	I	Pb	0.005	−1.0	1.0	12.0	
73	G^4	H	I	Pb	0.005	1.0	1.0	12.0	
74	G^4	H	I	Pb	0.005	1.0	4.0	12.0	
75	G^2	C	H		0.004			12.0	0.0
76	G^2	C	H		0.028			12.0	0.0
77	G^2	C	H		0.139			12.0	0.0

no.	type	atom i	atom j	atom k	η(1/Bohr^2)	λ	ζ	R_c(Bohr)	R_s(Bohr)
78	G^2	C	H		0.556			12.0	0.0
79	G^2	C	H		1.000			12.0	0.0
80	G^2	C	C		0.004			12.0	0.0
81	G^2	C	C		0.028			12.0	0.0
82	G^2	C	C		0.139			12.0	0.0
83	G^2	C	N		0.004			12.0	0.0
84	G^2	C	N		0.028			12.0	0.0
85	G^2	C	N		0.139			12.0	0.0
86	G^2	C	N		0.556			12.0	0.0
87	G^2	C	N		1.000			12.0	0.0
88	G^2	C	I		0.004			12.0	0.0
89	G^2	C	I		0.028			12.0	0.0
90	G^2	C	I		0.139			12.0	0.0
91	G^2	C	Pb		0.004			12.0	0.0
92	G^2	C	Pb		0.028			12.0	0.0
93	G^2	C	Pb		0.139			12.0	0.0
94	G^4	C	H	H	0.005	−1.0	1.0	12.0	
95	G^4	C	H	H	0.005	−1.0	4.0	12.0	
96	G^4	C	H	H	0.005	1.0	1.0	12.0	
97	G^4	C	H	H	0.005	1.0	4.0	12.0	
98	G^4	C	H	C	0.005	−1.0	1.0	12.0	
99	G^4	C	H	C	0.005	−1.0	4.0	12.0	
100	G^4	C	H	C	0.005	1.0	1.0	12.0	
101	G^4	C	H	C	0.005	1.0	4.0	12.0	
102	G^4	C	H	N	0.005	−1.0	1.0	12.0	
103	G^4	C	H	N	0.005	−1.0	4.0	12.0	
104	G^4	C	H	N	0.005	1.0	1.0	12.0	
105	G^4	C	H	N	0.005	1.0	4.0	12.0	
106	G^4	C	H	I	0.005	−1.0	1.0	12.0	
107	G^4	C	H	I	0.005	−1.0	4.0	12.0	
108	G^4	C	H	I	0.005	1.0	1.0	12.0	
109	G^4	C	H	I	0.005	1.0	4.0	12.0	
110	G^4	C	H	Pb	0.005	−1.0	1.0	12.0	
111	G^4	C	H	Pb	0.005	−1.0	4.0	12.0	
112	G^4	C	H	Pb	0.005	1.0	1.0	12.0	
113	G^4	C	H	Pb	0.005	1.0	4.0	12.0	
114	G^4	C	C	N	0.005	−1.0	1.0	12.0	
115	G^4	C	C	N	0.005	−1.0	4.0	12.0	
116	G^4	C	C	N	0.005	1.0	1.0	12.0	
117	G^4	C	C	N	0.005	1.0	4.0	12.0	
118	G^4	C	C	I	0.005	−1.0	1.0	12.0	
119	G^4	C	C	I	0.005	1.0	1.0	12.0	
120	G^4	C	C	I	0.005	1.0	4.0	12.0	
121	G^4	C	N	N	0.005	−1.0	1.0	12.0	
122	G^4	C	N	N	0.005	−1.0	4.0	12.0	

no.	type	atom i	atom j	atom k	η(1/Bohr^2)	λ	ζ	R_c(Bohr)	R_s(Bohr)
123	G^4	C	N	N	0.005	1.0	1.0	12.0	
124	G^4	C	N	I	0.005	−1.0	1.0	12.0	
125	G^4	C	N	I	0.005	−1.0	4.0	12.0	
126	G^4	C	N	I	0.005	1.0	1.0	12.0	
127	G^4	C	N	I	0.005	1.0	4.0	12.0	
128	G^4	C	N	Pb	0.005	−1.0	1.0	12.0	
129	G^4	C	N	Pb	0.005	−1.0	4.0	12.0	
130	G^4	C	N	Pb	0.005	1.0	1.0	12.0	
131	G^4	C	I	I	0.005	−1.0	1.0	12.0	
132	G^4	C	I	I	0.005	1.0	1.0	12.0	
133	G^4	C	I	I	0.005	1.0	4.0	12.0	
134	G^4	C	I	Pb	0.005	−1.0	1.0	12.0	
135	G^4	C	I	Pb	0.005	1.0	1.0	12.0	
136	G^4	C	I	Pb	0.005	1.0	4.0	12.0	
137	G^2	N	H		0.004			12.0	0.0
138	G^2	N	H		0.028			12.0	0.0
139	G^2	N	H		0.139			12.0	0.0
140	G^2	N	H		0.556			12.0	0.0
141	G^2	N	H		1.000			12.0	0.0
142	G^2	N	C		0.004			12.0	0.0
143	G^2	N	C		0.028			12.0	0.0
144	G^2	N	C		0.139			12.0	0.0
145	G^2	N	C		0.556			12.0	0.0
146	G^2	N	C		1.000			12.0	0.0
147	G^2	N	N		0.004			12.0	0.0
148	G^2	N	N		0.028			12.0	0.0
149	G^2	N	I		0.004			12.0	0.0
150	G^2	N	I		0.028			12.0	0.0
151	G^2	N	I		0.139			12.0	0.0
152	G^2	N	Pb		0.004			12.0	0.0
153	G^2	N	Pb		0.028			12.0	0.0
154	G^4	N	H	H	0.005	−1.0	1.0	12.0	
155	G^4	N	H	H	0.005	−1.0	4.0	12.0	
156	G^4	N	H	H	0.005	1.0	1.0	12.0	
157	G^4	N	H	H	0.005	1.0	4.0	12.0	
158	G^4	N	H	C	0.005	−1.0	1.0	12.0	
159	G^4	N	H	C	0.005	−1.0	4.0	12.0	
160	G^4	N	H	C	0.005	1.0	1.0	12.0	
161	G^4	N	H	C	0.005	1.0	4.0	12.0	
162	G^4	N	H	N	0.005	−1.0	1.0	12.0	
163	G^4	N	H	N	0.005	1.0	1.0	12.0	
164	G^4	N	H	N	0.005	1.0	4.0	12.0	
165	G^4	N	H	I	0.005	−1.0	1.0	12.0	
166	G^4	N	H	I	0.005	−1.0	4.0	12.0	
167	G^4	N	H	I	0.005	1.0	1.0	12.0	

no.	type	atom i	atom j	atom k	$\eta(1/\mathrm{Bohr}^2)$	λ	ζ	R_c(Bohr)	R_s(Bohr)
168	G^4	N	H	I	0.005	1.0	4.0	12.0	
169	G^4	N	H	Pb	0.005	−1.0	1.0	12.0	
170	G^4	N	H	Pb	0.005	1.0	1.0	12.0	
171	G^4	N	H	Pb	0.005	1.0	4.0	12.0	
172	G^4	N	C	C	0.005	−1.0	1.0	12.0	
173	G^4	N	C	C	0.005	−1.0	4.0	12.0	
174	G^4	N	C	C	0.005	1.0	1.0	12.0	
175	G^4	N	C	C	0.005	1.0	4.0	12.0	
176	G^4	N	C	N	0.005	1.0	1.0	12.0	
177	G^4	N	C	N	0.005	1.0	4.0	12.0	
178	G^4	N	C	I	0.005	−1.0	1.0	12.0	
179	G^4	N	C	I	0.005	−1.0	4.0	12.0	
180	G^4	N	C	I	0.005	1.0	1.0	12.0	
181	G^4	N	C	I	0.005	1.0	4.0	12.0	
182	G^4	N	C	Pb	0.005	−1.0	1.0	12.0	
183	G^4	N	C	Pb	0.005	1.0	1.0	12.0	
184	G^4	N	C	Pb	0.005	1.0	4.0	12.0	
185	G^4	N	N	I	0.005	1.0	1.0	12.0	
186	G^4	N	N	I	0.005	1.0	4.0	12.0	
187	G^4	N	I	I	0.005	−1.0	1.0	12.0	
188	G^4	N	I	I	0.005	1.0	1.0	12.0	
189	G^4	N	I	I	0.005	1.0	4.0	12.0	
190	G^4	N	I	Pb	0.005	−1.0	1.0	12.0	
191	G^4	N	I	Pb	0.005	1.0	1.0	12.0	
192	G^4	N	I	Pb	0.005	1.0	4.0	12.0	
193	G^2	I	H		0.004			12.0	0.0
194	G^2	I	H		0.028			12.0	0.0
195	G^2	I	H		0.139			12.0	0.0
196	G^2	I	C		0.004			12.0	0.0
197	G^2	I	C		0.028			12.0	0.0
198	G^2	I	C		0.139			12.0	0.0
199	G^2	I	N		0.004			12.0	0.0
200	G^2	I	N		0.028			12.0	0.0
201	G^2	I	N		0.139			12.0	0.0
202	G^2	I	I		0.004			12.0	0.0
203	G^2	I	I		0.028			12.0	0.0
204	G^2	I	Pb		0.004			12.0	0.0
205	G^2	I	Pb		0.028			12.0	0.0
206	G^2	I	Pb		0.139			12.0	0.0
207	G^4	I	H	H	0.005	−1.0	1.0	12.0	
208	G^4	I	H	H	0.005	−1.0	4.0	12.0	
209	G^4	I	H	H	0.005	1.0	1.0	12.0	
210	G^4	I	H	H	0.005	1.0	4.0	12.0	
211	G^4	I	H	C	0.005	−1.0	1.0	12.0	
212	G^4	I	H	C	0.005	−1.0	4.0	12.0	

no.	type	atom i	atom j	atom k	$\eta(1/\mathrm{Bohr}^2)$	λ	ζ	R_c(Bohr)	R_s(Bohr)
213	G^4	I	H	C	0.005	1.0	1.0	12.0	
214	G^4	I	H	C	0.005	1.0	4.0	12.0	
215	G^4	I	H	N	0.005	−1.0	1.0	12.0	
216	G^4	I	H	N	0.005	−1.0	4.0	12.0	
217	G^4	I	H	N	0.005	1.0	1.0	12.0	
218	G^4	I	H	N	0.005	1.0	4.0	12.0	
219	G^4	I	H	I	0.005	−1.0	1.0	12.0	
220	G^4	I	H	I	0.005	1.0	1.0	12.0	
221	G^4	I	H	I	0.005	1.0	4.0	12.0	
222	G^4	I	H	Pb	0.005	−1.0	1.0	12.0	
223	G^4	I	H	Pb	0.005	−1.0	4.0	12.0	
224	G^4	I	H	Pb	0.005	1.0	1.0	12.0	
225	G^4	I	H	Pb	0.005	1.0	4.0	12.0	
226	G^4	I	C	C	0.005	−1.0	1.0	12.0	
227	G^4	I	C	C	0.005	1.0	1.0	12.0	
228	G^4	I	C	C	0.005	1.0	4.0	12.0	
229	G^4	I	C	N	0.005	−1.0	1.0	12.0	
230	G^4	I	C	N	0.005	1.0	1.0	12.0	
231	G^4	I	C	N	0.005	1.0	4.0	12.0	
232	G^4	I	C	I	0.005	−1.0	1.0	12.0	
233	G^4	I	C	I	0.005	1.0	1.0	12.0	
234	G^4	I	C	I	0.005	1.0	4.0	12.0	
235	G^4	I	C	Pb	0.005	−1.0	1.0	12.0	
236	G^4	I	C	Pb	0.005	1.0	1.0	12.0	
237	G^4	I	C	Pb	0.005	1.0	4.0	12.0	
238	G^4	I	N	N	0.005	−1.0	1.0	12.0	
239	G^4	I	N	N	0.005	1.0	1.0	12.0	
240	G^4	I	N	I	0.005	−1.0	1.0	12.0	
241	G^4	I	N	I	0.005	1.0	1.0	12.0	
242	G^4	I	N	I	0.005	1.0	4.0	12.0	
243	G^4	I	N	Pb	0.005	−1.0	1.0	12.0	
244	G^4	I	N	Pb	0.005	1.0	1.0	12.0	
245	G^4	I	I	I	0.005	1.0	1.0	12.0	
246	G^4	I	I	Pb	0.005	−1.0	1.0	12.0	
247	G^4	I	I	Pb	0.005	1.0	1.0	12.0	
248	G^4	I	I	Pb	0.005	1.0	4.0	12.0	
249	G^4	I	Pb	Pb	0.005	−1.0	1.0	12.0	
250	G^4	I	Pb	Pb	0.005	1.0	1.0	12.0	
251	G^2	Pb	H		0.004			12.0	0.0
252	G^2	Pb	H		0.028			12.0	0.0
253	G^2	Pb	H		0.139			12.0	0.0
254	G^2	Pb	C		0.004			12.0	0.0
255	G^2	Pb	C		0.028			12.0	0.0
256	G^2	Pb	C		0.139			12.0	0.0
257	G^2	Pb	N		0.004			12.0	0.0

no.	type	atom i	atom j	atom k	$\eta(1/\mathrm{Bohr}^2)$	λ	ζ	R_c(Bohr)	R_s(Bohr)
258	G^2	Pb	N		0.028			12.0	0.0
259	G^2	Pb	I		0.004			12.0	0.0
260	G^2	Pb	I		0.028			12.0	0.0
261	G^2	Pb	I		0.139			12.0	0.0
262	G^2	Pb	Pb		0.004			12.0	0.0
263	G^2	Pb	Pb		0.028			12.0	0.0
264	G^4	Pb	H	H	0.005	−1.0	1.0	12.0	
265	G^4	Pb	H	H	0.005	1.0	1.0	12.0	
266	G^4	Pb	H	H	0.005	1.0	4.0	12.0	
267	G^4	Pb	H	C	0.005	−1.0	1.0	12.0	
268	G^4	Pb	H	C	0.005	1.0	1.0	12.0	
269	G^4	Pb	H	C	0.005	1.0	4.0	12.0	
270	G^4	Pb	H	N	0.005	1.0	1.0	12.0	
271	G^4	Pb	H	N	0.005	1.0	4.0	12.0	
272	G^4	Pb	H	I	0.005	−1.0	1.0	12.0	
273	G^4	Pb	H	I	0.005	1.0	1.0	12.0	
274	G^4	Pb	H	I	0.005	1.0	4.0	12.0	
275	G^4	Pb	C	N	0.005	1.0	1.0	12.0	
276	G^4	Pb	C	N	0.005	1.0	4.0	12.0	
277	G^4	Pb	C	I	0.005	−1.0	1.0	12.0	
278	G^4	Pb	C	I	0.005	1.0	1.0	12.0	
279	G^4	Pb	C	I	0.005	1.0	4.0	12.0	
280	G^4	Pb	N	I	0.005	−1.0	1.0	12.0	
281	G^4	Pb	N	I	0.005	1.0	1.0	12.0	
282	G^4	Pb	N	I	0.005	1.0	4.0	12.0	
283	G^4	Pb	I	I	0.005	−1.0	1.0	12.0	
284	G^4	Pb	I	I	0.005	−1.0	4.0	12.0	
285	G^4	Pb	I	I	0.005	1.0	1.0	12.0	
286	G^4	Pb	I	I	0.005	1.0	4.0	12.0	
287	G^4	Pb	I	Pb	0.005	−1.0	1.0	12.0	
288	G^4	Pb	I	Pb	0.005	1.0	1.0	12.0	
289	G^4	Pb	I	Pb	0.005	1.0	4.0	12.0	

3 DFT Settings

All DFT calculations were performed with the VASP [2, 3, 4, 5, 6] code using the strongly constrained and appropriately normed (SCAN) semilocal density functional meta-GGA [7]. A plane-wave basis set with a cutoff energy of 800 eV was used within the projector augmented wave (PAW) formalism. The basis set was constructed with Pb d-shell (14), I (7), N (5), C (4), H (1) electrons as valence states in the PAW potentials. The reciprocal space was sampled using Γ–centered k-grid meshes with spacings of 0.2 $\mathrm{Å}^{-1}$ and all calculations were spin unpolarized.

4 Order Parameter

To compute our order parameter, we first identify all PbI octahedra that are present. We then define three vectors $\vec{v}_{i\alpha}$ for each octahedron i, that connect two opposing iodine atoms in the direction of one of the three lattice vectors (index α). We then compute three order parameter values O_α by taking the mean of the absolute value of the dot product between nearest neighbor $\vec{v}_{i\alpha}$ pointing in the same direction α. Pairs of vectors pointing in two of the three directions are shown in Figure 8.

$$O_\alpha = \frac{1}{6N} \sum_i \sum_j \frac{|\vec{v}_{i\alpha} \cdot \vec{v}_{j\alpha}|}{\|\vec{v}_{i\alpha}\| \|\vec{v}_{j\alpha}\|} \tag{4}$$

Here the sum over i includes all N octahedra, while the sum over j only includes the nearest neighbor octahedra to i.

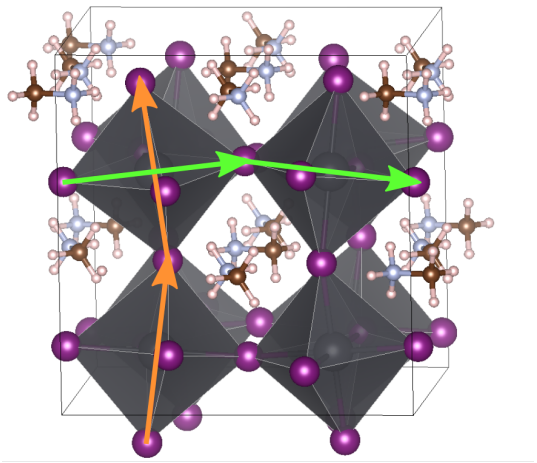

Supplemental Figure 8: Pairs of vectors used for computing the order parameters. Two pairs, pointing into the two directions parallel to the image plane are shown in green and orange.

5 Funnel Hopping Monte Carlo

5.1 Acceptance Rates of MC Moves

In Figure 9 and Figure 10, acceptance rates plotted against temperature and the parameter λ are shown. Since a 2D grid of replicas was used, the acceptance rates were averaged over all replicas at the same temperature or λ values. The acceptance rate of the Hamiltonian MC (HMC) moves are almost independent of the temperature and λ. The acceptance rate of the FHMC moves is, as expected, exactly 1 at $\lambda = 1$ and decays very rapidly for decreasing λ.

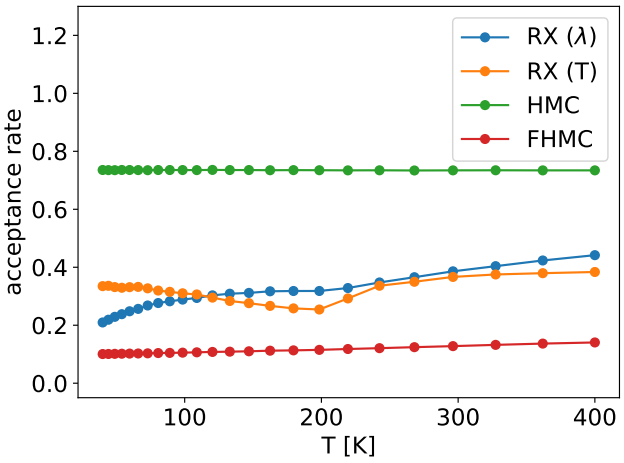

Supplemental Figure 9: Acceptance rate of the Hamiltonian MC Monte Carlo (HMC), Funnel Hopping Monte Carlo (FHMC) and replica exchange moves between replicas with different λ values (RX (λ)) and temperatures (RX (T)) plotted against temperature. The values shown are averages over all replicas with the same value of λ.

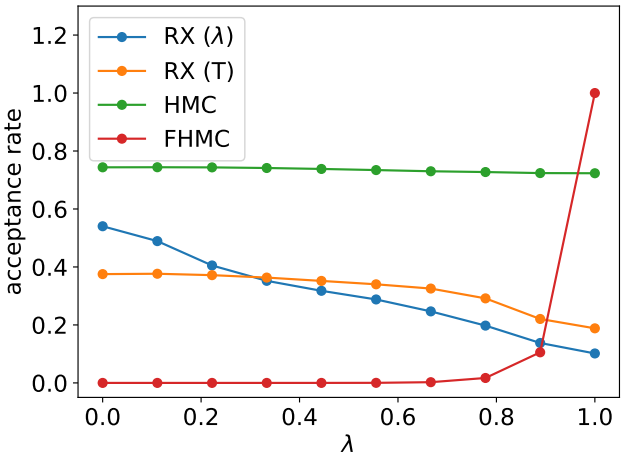

Supplemental Figure 10: Acceptance rate of the Hamiltonian MC Monte Carlo (HMC), funnel hopping Monte Carlo (FHMC) and replica exchange moves between replicas with different λ values (RX (λ)) and temperatures (RX (T)) plotted against λ. The values shown are averages over all replicas with the same temperature.

5.2 FHMC Simulation With a Different Lattice Parameters of the Tetragonal Phase

As mentioned in the main text, we observed a strong dependence of the tetragonal to cubic transition on the lattice parameters. We therefore ran FHMC simulations where the lattice parameters of the tetragonal phase were chosen as the average lattice parameters of an MD simulation at 250 K. The order parameters shown in Figure 11, show

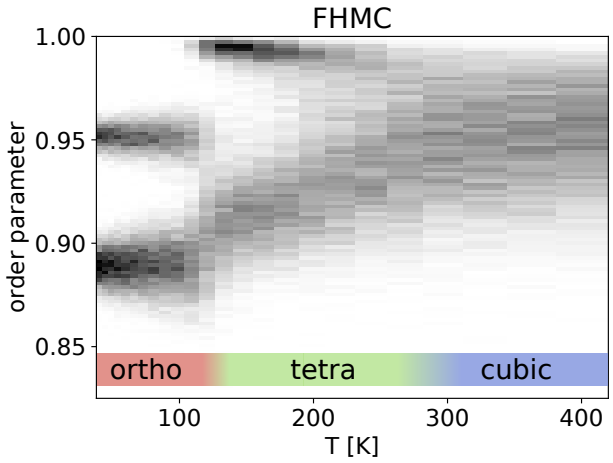

Supplemental Figure 11: Histogram of the order parameter versus temperature obtained from an FHMC simulation where the tetragonal lattice was slightly adjusted.

much closer agreement with the results obtained from MD.

6 Harmonic and Quasi Harmonic Approximation

We used phonopy [8] to compute the free energy of the different $MaPbI_3$ phases using the harmonic (HA) and quasi harmonic (QHA) approximation. The free energies were calculated using the same NNP based PES that was also used for our FHMC simulations. Due to the strong anharmonicity and large difference between the softest and hardest modes, computing the HA and QHA was challenging. The local minima were optimized using the vc-SQNM algorithm [9] to a maximum force value of 10^{-8} Ha/Bohr. Force constants were computed through finite differences with an extremely small displacements of 10^{-5} Å as larger displacements would result in imaginary phonon frequencies. Such small displacements are only possible because the NNP PES is a smooth function, that can be computed with almost machine precision. On a DFT PES, larger displacements would have to be used. For all phases, supercells consisting of 8 functional units, as shown in Section 1, were used. The relative free energies are shown in Figure 12 and the phonon densities of state are shown in Figure 13.

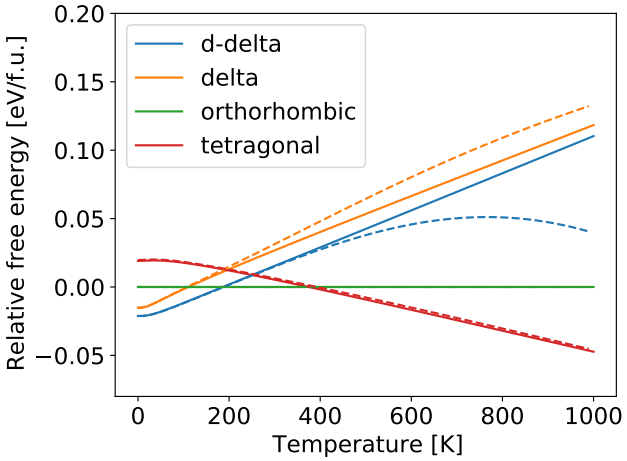

Supplemental Figure 12: Relative free energies computed with the HA (solid lines) and QHA (dashed lines) with respect to the orthorhombic phase.

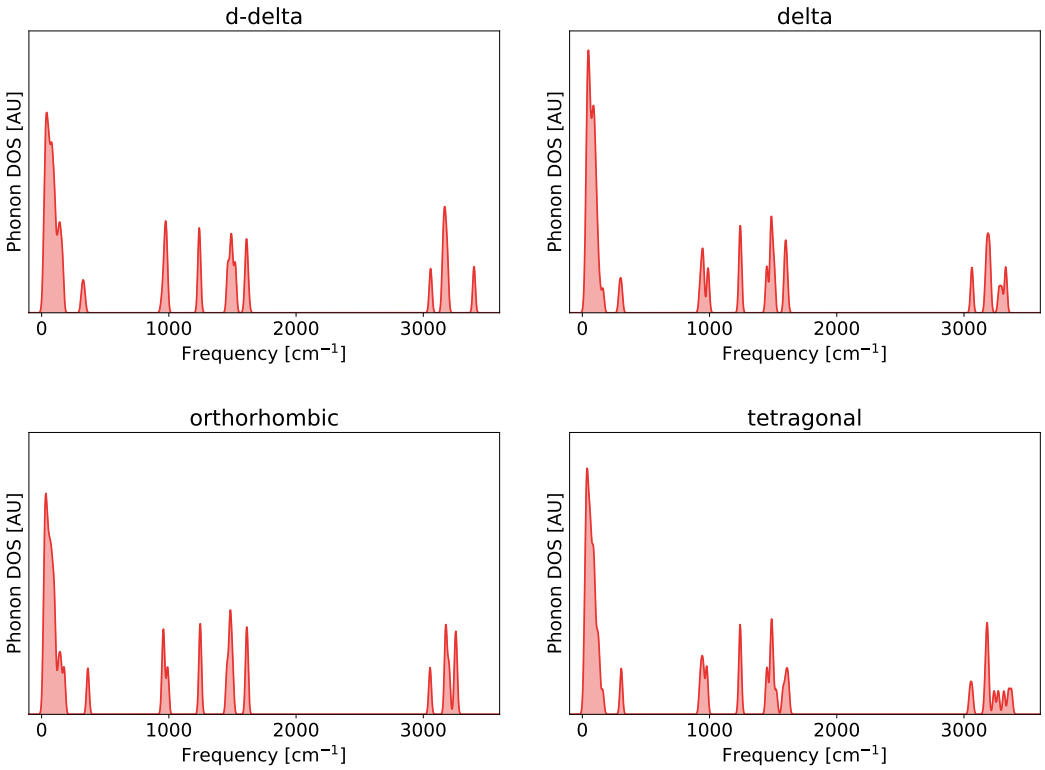

Supplemental Figure 13: Phonon density of states computed using the NNP and phonopy for all five $MaPbI_3$ phases. A convolution with a Gaussian function with a standard deviation of $10\,\mathrm{cm}^{-1}$ was used to obtain a smooth DOS.

Supplemental References

[1] J. Behler, *The Journal of chemical physics*, 2011, **134**, 074106.

[2] G. Kresse and J. Furthmüller, *Computational materials science*, 1996, **6**, 15–50.

[3] G. Kresse and J. Hafner, *Physical review B*, 1993, **47**, 558.

[4] G. Kresse and J. Furthmüller, *Physical review B*, 1996, **54**, 11169.

[5] G. Kresse and J. Hafner, *Journal of Physics: Condensed Matter*, 1994, **6**, 8245.

[6] G. Kresse and D. Joubert, *Physical review b*, 1999, **59**, 1758.

[7] J. Sun, A. Ruzsinszky and J. P. Perdew, *Physical review letters*, 2015, **115**, 036402.

[8] A. Togo and I. Tanaka, *Scr. Mater.*, 2015, **108**, 1–5.

[9] M. Gubler, M. Krummenacher, H. Huber and S. Goedecker, *arXiv preprint arXiv:2206.07339*, 2022.